

Learning to Grasp: from Somewhere to Anywhere

François Héli  on^{1†*}, Johann Huber^{1†}, Fa  z Ben Amar¹ and St  phane Doncieux¹

Abstract—Robotic grasping is still a partially solved, multidisciplinary problem where data-driven techniques play an increasing role. The sparse nature of rewards make the automatic generation of grasping datasets challenging, especially for unconventional morphologies or highly actuated end-effectors. Most approaches for obtaining large-scale datasets rely on numerous human-provided demonstrations or heavily engineered solutions that do not scale well. Recent advances in Quality-Diversity (QD) methods have investigated how to learn object grasping at a specific pose with different robot morphologies. The present work introduces a pipeline for adapting QD-generated trajectories to new object poses. Using an RGB-D data stream, the vision pipeline first detects the targeted object, predicts its 6-DOF pose, and finally tracks it. An automatically generated reach-and-grasp trajectory can then be adapted by projecting it relatively to the object frame. Hundreds of trajectories have been deployed into the real world on several objects and with different robotic setups: a Franka Research 3 with a parallel gripper and a UR5 with a dexterous SIH Schunk hand. The transfer ratio obtained when applying transformation to the object pose matches the one obtained when the object pose matches the simulation, demonstrating the efficiency of the proposed approach.

I. INTRODUCTION

While advances in deep learning have shown great progress in many artificially intelligent tasks such as vision, speech recognition, or language, learning robots still struggle to act in the real world. This work focuses on grasping, one of the most fundamental skills required by a robot to further interact with the world [2], especially when considering highly actuated, multi-fingered end-effectors such as robotic hands [3]. The ultimate goal of grasping is not only to apply forces to an object but also to fit into a more general sensory-rich and task-related process: what part of the object should be grasped to carry out the task? How should the robot approach the object to reach this specific part? How can grasping trajectories be adapted given sensory inputs?

As robotic interactions between hands and graspable objects are hard to model, sampling and data-driven techniques are often considered for learning grasp candidates. However, grasping rewards sparsity hinders traditional learning-based approaches for real-world application. Robotics is a data-scarce domain where exploration is difficult. To alleviate these issues, most approaches rely on priors, costly and time-consuming data collection from human demonstrations [4], [5], [6], limiting scalability and diversity of behaviors. Moreover, more investigations are needed when it comes to

the transferability of learned grasping policies with robotic hands in the real-world setting [3].

Recent works on Quality-Diversity (QD), a branch of evolutionary algorithms that select individuals that are both novel and performing [7]. It showed promising results on the automatic generation of reach-and-grasp trajectories [1]. QD methods aim to find solutions that are as diverse as possible in a given behavioral space. Then they optimize, in the vicinity of a particular behavior, for the best-performing individual given a performance criterion. In terms of grasping, this leads to optimizing for reach-and-grasp trajectories that explore efficiently **different ways** to grasp the object with robustness objectives. First applications demonstrated in simulation the ability to generate a highly diverse set of successful **open-loop** grasping trajectories, **without demonstration or supervision**, on various robotic arms and end-effectors **given the 3D model of an object and a simulated scene**. Recent works [8], further studied the simulation to the real gap and the transferability of the open-loop generated grasping trajectories at a specific object pose.

This article extends these prior works by proposing adapting the generated datasets to new object poses. We also propose a pipeline integrating state-of-the-art vision modules for real-world application of the adapted trajectories and tested it in challenging settings.

The provided contributions are the following:

- We propose an integration pipeline that leverages State-of-the-art vision modules and classical robotic motion planning to adapt a dataset of diverse open-loop grasping trajectories generated with a QD algorithm to new object poses;
- Experiments conducted on various real robots, objects, sensors, scenes, and end-effectors show that the proposed pipeline results in success ratios similar to the one reported in the literature when the object is positioned at the same pose as in the simulation – demonstrating the efficiency of the approach. (see Figure 1)
- Synthetic analysis shows that the adaptation of reach-and-grasp trajectories is able to adapt the grasps to new poses while maintaining the grasping diversity and, to a certain extent, the diversity of the pre-grasp approach.

The joint video presents the overall pipeline and experiments. The code for generating open-loop trajectories for a specific object pose is available on Github¹.

* corresponding author

† equal contributions

¹Sorbonne Universit  , CNRS, Institut des Syst  mes Intelligents et de Robotique, ISIR, F-75005 Paris, France {helenon, huber, benamar, doncieux}@isir.upmc.fr

¹<https://github.com/Johann-Huber/qd-grasp>

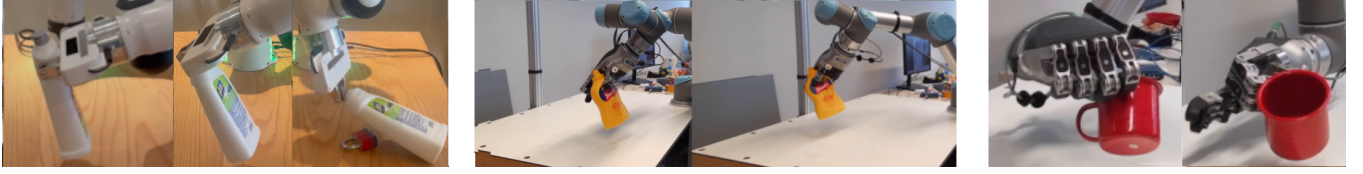


Fig. 1. The proposed method allows the adaptation of automatically generated reach-and-grasp trajectories to other object positions than the one used in the simulation to generate the grasps [1]. (Left) Diverse examples on the FR3 arm; (Center) A same trajectory deployed for two different object poses; (Right) Examples of affordances allowed by the diversity of the adapted trajectories.

II. RELATED WORKS

Many approaches were proposed in order to scale data for vision [9], [10], language [11], [12] or speech [13]. Collecting data for real robotics, particularly for hard exploration problems such as grasping, is more difficult. Several methods are being investigated for handling this issue. Some approaches use manual data annotation and teleoperation learning [14], [15] or self-supervision [16], which are usually robot specific, time-consuming and cost expensive. Some approaches rely on simulation [17], [18] with limited sim2real transfer analysis. Recent approaches leverage foundation vision and language models to guide robot action [19] or massive offline visual data augmentation through a large diffusion model [20]. However, these approaches are perception-oriented, resulting into constrained operational space (e.g. top-down movements with parallel grippers). Automatic generation of diverse actions and for various end-effectors remains rare. In [21], the authors propose a data augmentation technique for rope manipulation attached to the end-effector based on rigid transforms but do not address how to approach and grasp the rope.

Relying on an automatically generated dataset of reach-and-grasp trajectory built with Quality-Diversity (QD) methods [1], we propose an integrated pipeline for data augmentation of the learned grasping trajectories compatible with new object poses.

III. METHOD

This section presents the proposed pipeline (Figure 2). Given an object model, a robot model, and an RGB-D camera, the goal is to adapt a dataset of diverse trajectories generated automatically by QD methods to new object poses.

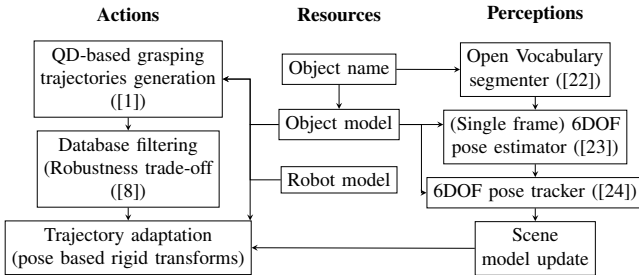


Fig. 2. Overview of the integration pipeline.

A. Problem definition and notations

Figure 3 defines the frames relevant to the problem definition. The example illustrates a UR5 with a dexterous hand and can be generalized to other manipulators, as demonstrated in section IV. B is the frame associated with the base of the robot fixed with respect to the world frame W , E with the end-effector, C with the camera, O_{ref} the object reference frame, which is the same as the one used in simulation, and O_{target} the actual, real-world, estimated frame of the object.

A reach-and-grasp trajectory τ for object reference follows a sequence of points in joint space $q_{0 \leq k \leq g}$, evenly spaced in time and where g is the index corresponding to grasping. Any point $q_{0 \leq k \leq g}$ is related to the frame $E_{0 \leq k \leq g}$ in the Cartesian space of the end-effector by the forward kinematics of the robotic arm. The problem can then be formulated as follows: Given an object initially at O_{ref} and a calibrated camera sensor, how can we build and adapt a large and diverse dataset of grasping trajectories for different object poses at O_{target} ?

We note ${}_{A1}^{A2}T$ the transform from frame $A2$ to frame $A1$. Given two transforms ${}_{A1}^{A2}T$ and ${}_{A2}^{A3}T$, the transform between $A1$ and $A3$ can be expressed as ${}_{A1}^{A2}T {}_{A2}^{A3}T = {}_{A1}^{A3}T$. Moreover ${}_{A2}^{A1}T = {}_{A1}^{A2}T^{-1}$. We suppose that the transform between the camera and the robot base ${}_B^CT$ is known. It can be computed, for instance, by hand-eye calibration.

B. Trajectory adaptation

As a first step, a simulation of the scene is generated in a physical simulator with the object at a location ${}_{B}^{O_{ref}}T$ and other potential colliding objects such as a table. A repertoire of diverse, open-loop grasping trajectories $\tau_{i \in \mathbb{N}}^O$ in joint space is generated by a Quality-Diversity (QD) algorithms [1]. This dataset goes through a filtering application $f : \tau^O \rightarrow f_n(\tau^O)$ based on general, physically informed quality metrics and domain randomization [8]. The resulting dataset D_{open}^O contains diverse trajectories that are likely to transfer well when the real object is placed at ${}_{B}^{O_{ref}}T$, as in the simulation. Given a new 6DOF pose ${}_{B}^{O_{target}}T$, a trajectory $\tau_i^O \in D_{open}^O$ is then adapted through a two-steps process. The reference path is first rigidly transformed with respect to ${}_{B}^{O_{target}}T$. Secondly, a valid trajectory τ_i^{O*} following the new path is searched by relying on traditional collision-aware motion planning.

Given the filtered trajectory $\tau_{i \in \mathbb{N}}^O$, represented by the sequence of joint coordinates $q_{0 \leq k \leq g}$, we first compute through forward kinematics the sequence of Cartesian poses with

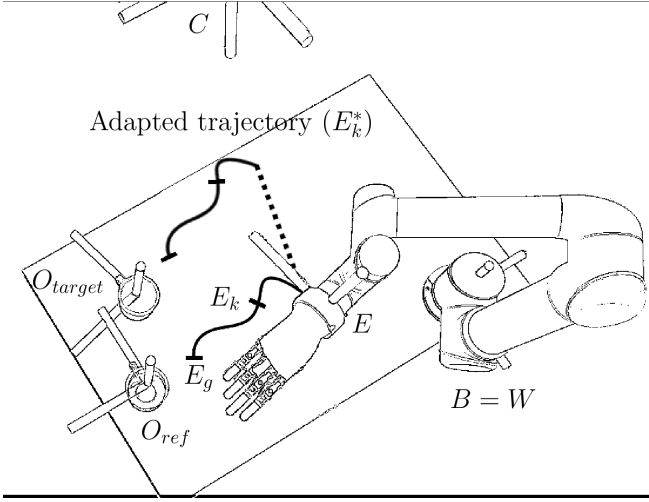


Fig. 3. **Notations and adaptation principle.** The visualization comes from the Rviz scene of the UR5 robot with the SIH dexterous hand. In this example, the robot has to grasp a mug (frame O_{target}) with a pose estimated by a RGB-D camera (frame C) and perceptual modules. The trajectories have been generated in simulation with the object at O_{ref} position. The path followed by the end-effector E is adapted from one pose to another. The robot end-effector follows the dotted line to reach the adapted path.

respect to the manipulator base: ${}^B_{E_{0 \leq k \leq g}} T$. In order to keep pregrasp approaches consistent for the new object pose, we enforce that the new trajectory must follow the same path relatively to the object pose: $\forall k, {}^{O_{target}}_{E_{0 \leq k \leq g}} T = {}^{O_{ref}}_{E_{0 \leq k \leq g}} T$. The reference path can be expressed with respect to the object reference frame ${}^{O_{ref}}_{E_{0 \leq k \leq g}} T = ({}^{O_{ref}}_B T)^{-1} {}^B_{E_{0 \leq k \leq g}} T$.

Hence ${}^B_{E_{0 \leq k \leq g}} T = {}^{O_{target}}_B T ({}^{O_{ref}}_B T)^{-1} {}^B_{E_{0 \leq k \leq g}} T$ with ${}^{O_{target}}_B T$ estimated from the camera (section III-C) and ${}^{O_{ref}}_B T$ from the simulation. Finally, new points are then interpolated between the intermediate poses ${}^B_{E_{0 \leq k \leq g}} T$. The new trajectory must be valid with respect to specific use case constraints $f_c(\tau_i^{O*})$. In our setting, $f_c(\tau_i^{O*}) = f_{IK}(\tau_i^{O*}) + f_{collision}(\tau_i^{O*})$, with f_{IK} assessing that the trajectory τ_i^{O*} is kinematically feasible with limited jump in joint space, and $f_{collision}$ assessing that no collisions happens between the robot and the environment or itself. Moveit! interfaces to the OMPL planner and the KDL kinematics solver are used for that purpose. Long trajectories are less likely to transfer as there are more risks of collision, reaching singularities, or moving outside the working space. In collision or invalid kinematics detection cases, the new path is iteratively truncated until index n until the planner finds a solution or rejection. The resulting truncated path is represented as the sequence of ${}^B_{E_{n \leq k \leq g}} T$ and leads to the final open-loop (truncated) trajectory $\tilde{\tau}_i^{O*}$. Time parameterization algorithms compute speed and acceleration profiles according to safety limits.

C. Object pose detection and tracking

In order to adapt the trajectory to real robots and collect data, a robust estimation of the object's pose ${}^{O_{target}}_B T$ is necessary. RGB-D cameras are promising sensors for that

purpose when it comes to real-world robots, as they are low-cost, easy to mount on the robot, and implicitly embed rich information about the world. Recently, vision research has seen significant advances in specific aspects of scene understanding given RGB and depth images. In this work, we propose an integrated three-step pipeline that is able to detect and track the 6DOF pose of an object, given its name and a known 3D mesh model. The right part of Figure 2 shows the overall visual perception pipeline. At first, we use *Detic* [22] a large **open-vocabulary object detector** based on deep neural networks (DNN) with pre-trained weights, without fine-tuning. Large open-vocabulary models are able to generalize to class names outside the learning dataset. Therefore, given an object name and an RGB image, *Detic* predicts bounding boxes and segmentation masks with a confidence level of the specific object to be grasped (see Figure 4).

The RGB and depth parts corresponding to the bounding box along with the 3D model of the object are then fed to *Megapose* [23] an **object pose detector** that predicts for a single image the 6DOF pose of the object. It does so in a two-step process. It first uses a *Render and Compare* strategy combined with a DNN classifier to predict the best matching pose given multiple random rendered views and the input RGB-D image. Then, a second multi-view rendering stage is performed by perturbing the coarse pose, and a second DNN classifier selects the best-refined pose. In this work, we used *Megapose* without fine-tuning, pre-trained models on synthetic data only. We finally leveraged *ICG* [24], an efficient 6DOF pose **tracker** (see Figure 5) that runs in real-time on CPU. It fuses depth modalities (ICP-based) and region modalities, relying on traditional and explainable tracking features such as lines, color histograms, geometry priors, and key points. We leveraged *Megapose* refined pose as a prior for the *ICG* tracker.

To summarize, our pipeline interfaces and exploits the advantages and disadvantages of the three modules. *Detic* detects objects given a class name taken from an open vocabulary, *Megapose* predicts a 6DOF pose from *Detic* detection, and *ICG* is responsible for tracking the 6DOF pose of the object. While *Detic* and *Megapose* heavily rely on GPU for inferences, *ICG* runs mostly on CPU, which gives more room to manage the computing hardware efficiently. Given a calibrated camera, *Megapose* and *ICG* express the object pose in the camera frame: ${}^C_{O_{target}} T$. For a camera fixed with respect to the robot base, hand-eye calibration gives ${}^C_B T$. It comes then that ${}^{O_{target}}_B T = {}^C_B T {}^C_{O_{target}} T$, and with results from section III-B everything is known for real-world applications.

IV. EXPERIMENTS

This section presents the experimental results of the proposed trajectory adaptation pipeline.

A. Platforms

Robots and scene: Experiments were completed on two different robots (Figure 6): a 6 degree of freedom (DOF)

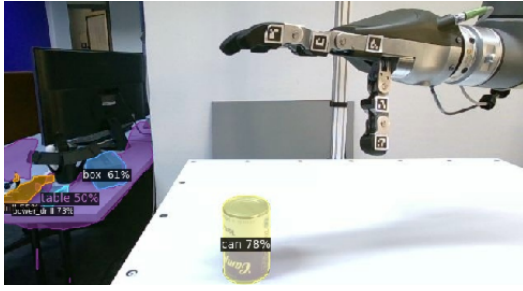


Fig. 4. **Object detection.** The open vocabulary module finds and segments relevant areas in the RGB image that match a queried object's name (the can in this example). The ArUco markers are not used in this experiment.

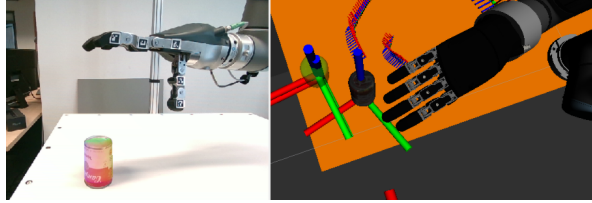


Fig. 5. **Object pose estimation.** Given a cropped RGB-D area, the 6DOF pose estimation [23] and tracking [24] modules are leveraged to update the current object pose estimate. (Left) The 3D model's estimated pose is transformed in the camera frame and overlaid with the real object; (Right) The reconstructed scene. The green and transparent mesh represents the tomato can be placed at O_{ref} , while the dense and dark mesh corresponds to the approximated pose of the object (attached to O_{target}).

Universal robot (UR5) and a 7 DOF Franka Research 3 (FR3). The FR3 gripper has parallel fingers with 1 DOF. The UR5 gripper is a SIH dexterous hand. Grasp learning and control of the SIH hand were made with synergies primitives (see Table I). The communication between the robot controller, camera sensors, and grippers is done through ROS. Each robot is mounted on a table, which is represented as a collision plane.

TABLE I
SIH HAND SYNERGIES

Fingers \ Hand synergy	Open	hs ₁	hs ₂	hs ₃	hs ₄
thumb		✓	✓	✓	✓
index		✓		✓	✓
mid			✓	✓	✓
ring and last					✓

Sensing: Experiments with the FR3 was conducted with a static Intel®RealSense™ Depth Camera D435i. Experiment with the UR5 and the dexterous hand was carried out alternatively with a RealSense D455 and a RealSense L515. Cameras were fixed at various mounting positions (Figure 6). All cameras were hand-eye calibrated with an ArUco marker.

Hardware compute specifications: Trajectory loading and transformations, 6DOF tracking processing, and control of robots were made on a DELL laptop (a 12 cores Intel® Core™ i7-10850H). Deep learning perceptual modules were run on a remote desktop PC with a dedicated GPU (Graphical Processing Unit), an Nvidia TITAN X 12GB for the FR3, and an NVIDIA RTX 2080 for the UR5. Moreover, the FR3

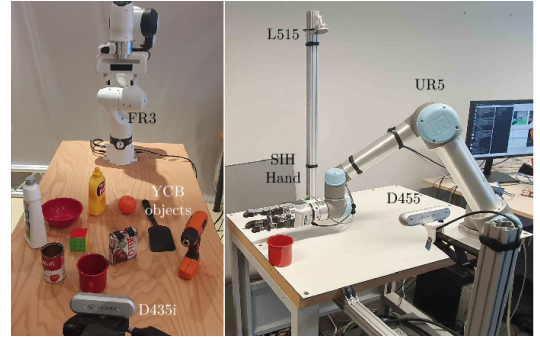


Fig. 6. **Experimental scenes.** (Left) A Franka Research 3 arm (7 DOF) with a parallel gripper is combined to a D435i RGB-D camera; (Right) A Universal UR5 robot (6 DOF) with an SIH Schunk 5-DOF hand. The L515 and the D455 RGB-D sensors were mounted on the same setup but were not used simultaneously. Both experiments involve the 10 YCB objects shown in the left picture.

robot required running the laptop with a real-time kernel.

Objects: Experiments were conducted on various YCB objects [25]. As the YCB objects' center of mass and inertia matrix were not correctly specified in the original dataset, we had to modify them in order to get a better transfer between the simulation and the real world.

Dataset generation: Data generation for pose-specific grasping trajectories was conducted on the Pybullet simulator [26]. ME-scs - a variant of MAP-Elites [27] - was used to generate the dataset as it has recently been shown that it is the most efficient QD method to generate large datasets of diverse grasps [1].

B. Trajectory adaptation analysis

In order to quantify the augmentation potential of the adapted trajectories, we first simulated trajectory adaptation for three objects (mug, power drill, and pudding box) in the FR3 scene. We defined a working space for the FR3 as a box in front of it. The working space was divided into equal-sized cells, defining different positions and orientations for the objects. For each object, five trajectories were randomly sampled and then adapted for each pose. We measured for each pose the number of trajectories that were successfully adapted (i.e., the planner found a solution). This gives an indicator for the ability to generate a diversity of grasping at several positions of the working space (Figure 7 and 8). We also measured how much of the original path was successfully adapted by computing the ratio between the number of non-truncated points and the number of points of the original trajectory $1 - \frac{n_{\text{TRUNCATED POINTS}}}{n_{\text{REFERENCE POINTS}}}$. This gives information on the ability to generate diversity for the reaching phase (Figure 9 and 10). A ratio close to 0 means that the robot directly aims toward the grasping pose. A ratio close to 1 means that the robot follows most of the adapted path without truncation and therefore keeps most of the diversity of the reference pregrasp approach.

From Figure 7, different properties of the adaptation emerge depending on the position of the object over the reachable space of the robot. All objects follow a similar

pattern. When objects are very close to the robot, or at the limit of the reachable space, risks of auto-collision and unfeasible kinematics make all grasping trajectories fail. As objects move closer to the center of the reachable space, more and more trajectories are found. We can notably observe the emergence of areas where only a subset of the trajectories are successful. This shows that maintaining a certain level of diversity during generation is important in order to always have at least one adapted trajectory that can grasp the object in those areas.

Figure 8 further illustrates the effects of orientation and height level on the adaptation for the mug. Large changes in orientation have a globally more negative impact than translation, as adapted trajectories are more likely to hit the table, go out of reachable space, or face infeasible kinematics. For instance, when the mug is knocked over, the handle is no longer accessible without touching the table. Hence, when the mug is translated in $+z$ direction, more successes are observed.

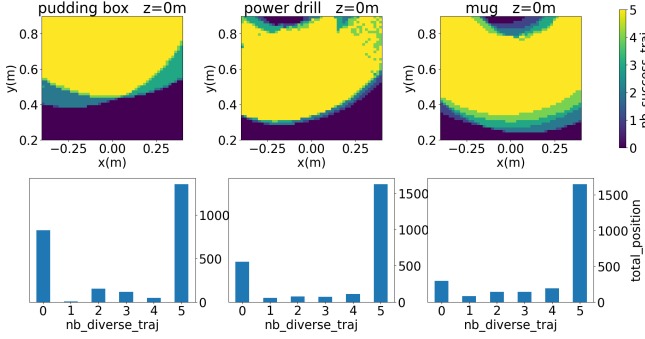


Fig. 7. How many trajectories can the robot follow to grasp the targeted object at different Cartesian positions? Each object (pudding box, power drill, mug) is virtually translated, without rotations, in the $(x,y,0)$ plane at around 2500 positions. The top row shows the number of trajectories successfully adapted for each position. The bottom plots show the number of positions for which diverse trajectories have been successfully adapted. The robot base is positioned at $(0,0,0)$ and faces the $+y$ direction.

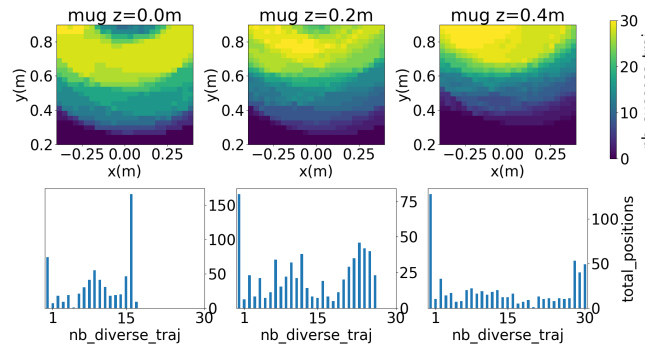


Fig. 8. Adaption to translated and rotated objects. The mug is now virtually rotated (6 orientations) and translated (1875 positions) into the (x,y,z) volume. (Top row) Number of trajectories that were successfully adapted for each position – results for different orientations are aggregated for a given position; (Bottom row) Number of positions for which diverse trajectories have been successfully adapted.

While previous analysis demonstrates that it is possible

to adapt diverse grasping poses, Figure 9 and 10 focus on the adaptation of the reaching part of the trajectory. The evolution of the truncation ratio shows that for large areas in the working space, there are trajectories for which it is possible to keep between 20% and 100% of the trajectories. It is highly dependent on the object and the type of trajectory. For instance, the sampled trajectories for the pudding box were almost straight in the Cartesian space, and therefore, most of the path has been kept, while some of the sampled trajectories for the power drill followed paths with large movements (see the video), leading parts of the path out of the reachable space.

Overall, the adaptation method can find at least one trajectory, most of the time, for most of the object poses, while maintaining diversity for both the grasping pose and the pregrasp approach. From only 5 diverse trajectories per object, it has been possible to generate thousands of adapted reach-and-grasp trajectories for a large area in the working space.

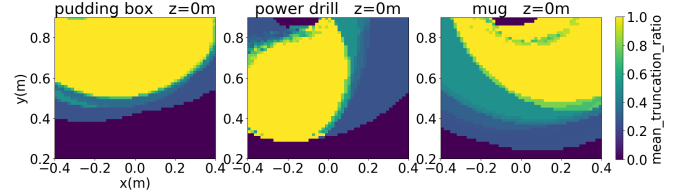


Fig. 9. How long is the robot able to follow the reference trajectory? Mean truncation ratio of all successful trajectories at a given position (Same experiment as in Figure 7.)

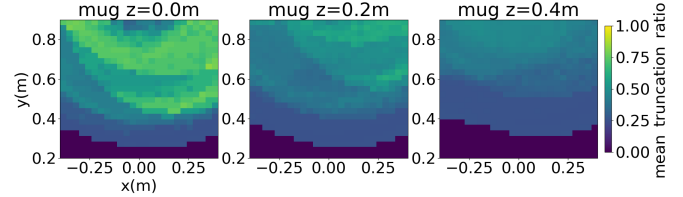


Fig. 10. How long is the robot able to follow the reference trajectory? Mean truncation ratio of all successful trajectories at a given position (Same experiment as in Figure 8.)

V. INTEGRATED PIPELINE RESULTS AND DISCUSSION

For each object, we randomly sampled trajectories promoting diversity at various positions and orientations in the working space. And each trajectory was tested with the object moved at different locations. Overall, we collected 300 trajectories on the different setups. For pose detection, we first give the name of the object to the semantic module, which then feeds the 6DOF pose estimation module with the cropped RGB-D data. Depending on initialization and the current view of the object, visual ambiguities can lead to the wrong initial pose estimation. To mitigate this limitation, we oriented objects so that several faces are in the field of view of the camera, and we reinitialized the initial pose estimation if necessary. Then, by leveraging the 6DOF tracker, we

placed the object at the target location. A GUI was developed to ease monitoring the overall process (see the video).

Figure 11 shows the success rate of adapted grasping trajectories for all the tested setups. Most objects, even complex ones such as the power drill, show a grasp success rate of over 50%. The average success ratio is around 60%, which is comparable to the obtained transferability ratio when the object pose matches the one in the simulation [8]. The most challenging objects are the bowl, the orange, and the spatula, primarily because of vision failure. Figure 12 illustrates one example of failure modes that were observed for the power drill. As we use a single view, the partial point cloud is not always enough to disambiguate the pose. Furthermore, the depth measurements might also be too noisy, especially for objects small or far from the camera, leading to wrong position or orientation predictions when 6DOF modules fall into local optima. This is especially true for objects with symmetries, such as the bowl and the orange, for which it is difficult to find the right orientation.

Transferability failures can also emerge from the base dataset. Simulation exploitation can still lead to trajectories that are valid in simulation but impossible or underperforming in reality. For instance, as contact simulation is usually far from reality, some reach-and-grasp trajectories led to slippery grasps that could succeed or fail depending on the estimated pose noise. For instance, the orange’s low adherent plastic, combined with its ball shape, makes grasping with two fingers very difficult. Depending on the amount of grasping force, the orange tends to be expelled from the parallel finger grasp. Moreover, as we promoted diversity in the grasping process, some trajectories were naturally less robust than others. For instance, grasping the mug by the handle is more difficult than grasping the surface of the mug. For tasks where only robust grasping is relevant, the filtering process of the initial dataset can be reinforced.

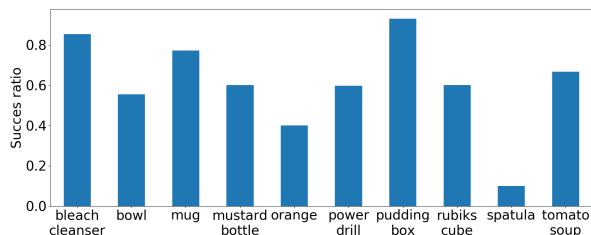


Fig. 11. **Success ratios.** Ratio of reach-and-grasp trajectories that have been successfully adapted on the 2 real robots.

VI. CONCLUSION

This paper proposes a novel method for learning to grasp an object at any pose. For that purpose, given a model of the object and the robot, a Quality-Diversity algorithm generates a **dataset of diverse open-loop trajectories**. The dataset is further **augmented** by rigid transforms with respect to new object poses and constraints based on collision avoidance and kinematics constraints. In order to demonstrate transfer in the

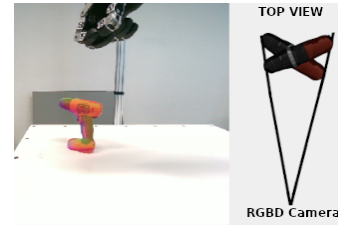


Fig. 12. **Object pose ambiguities.** Ambiguities appear depending on the view, the object, and the distance to the camera. Here, the power drill is too far from the camera. Depth measurements are not able to solve ambiguities. The predicted orientation is wrong over the z-axis.

real world, **an entire pipeline** integrating **actions** and state-of-the-art 6DOF object **perception** modules based on low-cost RGB-D cameras was developed. The generality of the approach was assessed by learning and deploying **hundreds of successful trajectories** on very **different objects and setups** including the use of a **dexterous hand**.

There are still limitations at various stages of the proposed pipeline, which lead to future work directions. Most failures are related to faulty 6DOF perception, especially when objects are too close, too far, or ambiguously oriented with respect to the camera. Leveraging multi-view perception based on multiple cameras or a single wrist-mounted, moving camera could help improve 6DOF perception and trajectory adaptation transfer. Moreover, the current approach requires a model of the object. Depending on the application context, real robots are likely to face novel objects without a known 3D model. Integrating on-the-fly object volumetric reconstruction, such as NerF-based techniques [28], could be a promising way for adaptation to many unknown situations. Finally, the diversity of generated trajectories can be used as a powerful exploration mechanism. Several techniques based on Reinforcement Learning still struggle with hard exploration problems such as grasping. Future work will also investigate how the resulting dataset can be leveraged to bootstrap RL learning algorithms in closed-loop, visual-servoing settings.

VII. ACKNOWLEDGEMENT

This work was supported by the Sorbonne Center for Artificial Intelligence, the German Ministry of Education and Research (BMBF) (01IS21080), and the French Agence Nationale de la Recherche (ANR) (ANR-21-FAI1-0004) - Learn2Grasp. It has received funding from the European Commission’s Horizon Europe Framework Programme under grant agreement No 101070381 and from the European Union’s Horizon Europe Framework Programme under grant agreement No 101070596. This work was performed using HPC resources from GENCI-IDRIS (Grant 20XX-AD011014320). Authors deeply thank Pr. Sven Behnke and the members of the AIS lab of Bonn for their warm welcome and support with the UR5 and SIH setup.

REFERENCES

- [1] J. Huber, F. H  l  non, M. Coninx, F. B. Amar, and S. Doncieux, "Quality Diversity under Sparse Reward and Sparse Interaction: Application to Grasping in Robotics," July 2023, arXiv preprint.
- [2] R. Hodson, "How robots are grasping the art of gripping," *Nature*, vol. 557, no. 7704, pp. S23–S25, May 2018.
- [3] Y. Li, P. Wang, R. Li, M. Tao, Z. Liu, and H. Qiao, "A Survey of Multifingered Robotic Manipulation: Biological Results, Structural Evolutions, and Learning Methods," *Frontiers in Neurorobotics*, vol. 16, 2022.
- [4] P. Wang, F. Manhardt, L. Minciullo, L. Garattoni, S. Meier, N. Navab, and B. Busam, "DemoGrasp: Few-Shot Learning for Robotic Grasping with Human Demonstration," in *2021 IEEE/RSJ International Conference on Intelligent Robots and Systems (IROS)*, Sept. 2021, pp. 5733–5740.
- [5] A. Brohan, N. Brown, J. Carbajal, Y. Chebotar, J. Dabis, C. Finn, K. Gopalakrishnan, K. Hausman, A. Herzog, J. Hsu, J. Ibarz, B. Ichter, A. Irpan, T. Jackson, S. Jesmonth, N. Joshi, R. Julian, D. Kalashnikov, Y. Kuang, I. Leal, K.-H. Lee, S. Levine, Y. Lu, U. Malla, D. Manjunath, I. Mordatch, O. Nachum, C. Parada, J. Peralta, E. Perez, K. Pertsch, J. Quiambao, K. Rao, M. Ryoo, G. Salazar, P. Sanketi, K. Sayed, J. Singh, S. Sontakke, A. Stone, C. Tan, H. Tran, V. Vanhoucke, S. Vega, Q. Vuong, F. Xia, T. Xiao, P. Xu, S. Xu, T. Yu, and B. Zitkovich, "RT-1: Robotics Transformer for Real-World Control at Scale," in *Robotics: Science and Systems XIX*. Robotics: Science and Systems Foundation, July 2023.
- [6] J. Ye, J. Wang, B. Huang, Y. Qin, and X. Wang, "Learning Continuous Grasping Function with a Dexterous Hand from Human Demonstrations," Mar. 2023.
- [7] A. Cully, J.-B. Mouret, and S. Doncieux, "Quality-diversity optimisation," in *Proceedings of the Genetic and Evolutionary Computation Conference Companion*, ser. GECCO '22. New York, NY, USA: Association for Computing Machinery, July 2022, pp. 864–889.
- [8] J. Huber, F. Helenon, F. Ben Amar, and S. Doncieux, "Domain Randomization for Sim2real Transfer of Automatically Generated Grasping Datasets," September 2023, arXiv preprint.
- [9] A. Dosovitskiy, L. Beyer, A. Kolesnikov, D. Weissenborn, X. Zhai, T. Unterthiner, M. Dehghani, M. Minderer, G. Heigold, S. Gelly, J. Uszkoreit, and N. Houlsby, "An Image is Worth 16x16 Words: Transformers for Image Recognition at Scale," June 2021.
- [10] J.-B. Alayrac, J. Donahue, P. Luc, A. Miech, I. Barr, Y. Hasson, K. Lenc, A. Mensch, K. Millican, M. Reynolds, R. Ring, E. Rutherford, S. Cabi, T. Han, Z. Gong, S. Samangooei, M. Monteiro, J. Menick, S. Borgeaud, A. Brock, A. Nematzadeh, S. Sharifzadeh, M. Binkowski, R. Barreira, O. Vinyals, A. Zisserman, and K. Simonyan, "Flamingo: A Visual Language Model for Few-Shot Learning," Nov. 2022.
- [11] T. B. Brown, B. Mann, N. Ryder, M. Subbiah, J. Kaplan, P. Dhariwal, A. Neelakantan, P. Shyam, G. Sastry, A. Askell, S. Agarwal, A. Herbert-Voss, G. Krueger, T. Henighan, R. Child, A. Ramesh, D. M. Ziegler, J. Wu, C. Winter, C. Hesse, M. Chen, E. Sigler, M. Litwin, S. Gray, B. Chess, J. Clark, C. Berner, S. McCandlish, A. Radford, I. Sutskever, and D. Amodei, "Language Models are Few-Shot Learners," July 2020.
- [12] J. Devlin, M.-W. Chang, K. Lee, and K. Toutanova, "BERT: Pre-training of Deep Bidirectional Transformers for Language Understanding," May 2019.
- [13] A. Radford, J. W. Kim, T. Xu, G. Brockman, C. McLeavey, and I. Sutskever, "Robust Speech Recognition via Large-Scale Weak Supervision,"
- [14] P. Shukla, N. Pramanik, D. Mehta, and G. C. Nandi, "GI-NNet & RGI-NNet: Development of Robotic Grasp Pose Models, Trainable with Large as well as Limited Labelled Training Datasets, under supervised and semi supervised paradigms," July 2021.
- [15] A. Mandlekar, J. Booher, M. Spero, A. Tung, A. Gupta, Y. Zhu, A. Garg, S. Savarese, and L. Fei-Fei, "Scaling Robot Supervision to Hundreds of Hours with RoboTurk: Robotic Manipulation Dataset through Human Reasoning and Dexterity," Nov. 2019.
- [16] S. Dasari, F. Ebert, S. Tian, S. Nair, B. Bucher, K. Schmeckpeper, S. Singh, S. Levine, and C. Finn, "RoboNet: Large-Scale Multi-Robot Learning," Jan. 2020.
- [17] C. Eppner, A. Mousavian, and D. Fox, "ACRONYM: A Large-Scale Grasp Dataset Based on Simulation," in *2021 IEEE International Conference on Robotics and Automation (ICRA)*, May 2021, pp. 6222–6227.
- [18] D. Turpin, T. Zhong, S. Zhang, G. Zhu, J. Liu, R. Singh, E. Heiden, M. Macklin, S. Tsogkas, S. Dickinson, and A. Garg, "Fast-Grasp'D: Dexterous Multi-finger Grasp Generation Through Differentiable Simulation," June 2023.
- [19] J. Yang, W. Tan, C. Jin, B. Liu, J. Fu, R. Song, and L. Wang, "Pave the Way to Grasp Anything: Transferring Foundation Models for Universal Pick-Place Robots," June 2023.
- [20] T. Yu, T. Xiao, A. Stone, J. Tompson, A. Brohan, S. Wang, J. Singh, C. Tan, D. M. J. Peralta, B. Ichter, K. Hausman, and F. Xia, "Scaling Robot Learning with Semantically Imagined Experience," Feb. 2023.
- [21] P. Mitrano and D. Berenson, "Data Augmentation for Manipulation," in *Robotics: Science and Systems XVIII*. Robotics: Science and Systems Foundation, June 2022.
- [22] X. Zhou, R. Girdhar, A. Joulin, P. Kr  henb  hl, and I. Misra, "Detecting Twenty-Thousand Classes Using Image-Level Supervision," in *Computer Vision – ECCV 2022*, S. Avidan, G. Brostow, M. Ciss  , G. M. Farinella, and T. Hassner, Eds. Cham: Springer Nature Switzerland, 2022, vol. 13669, pp. 350–368.
- [23] Y. Labb  , L. Manuelli, A. Mousavian, S. Tyree, S. Birchfield, J. Tremblay, J. Carpentier, M. Aubry, D. Fox, and J. Sivic, "MegaPose: 6D Pose Estimation of Novel Objects via Render & Compare," in *6th Annual Conference on Robot Learning*, Aug. 2022.
- [24] M. Stoiber, M. Sundermeyer, and R. Triebel, "Iterative Corresponding Geometry: Fusing Region and Depth for Highly Efficient 3D Tracking of Textureless Objects," in *2022 IEEE/CVF Conference on Computer Vision and Pattern Recognition (CVPR)*. New Orleans, LA, USA: IEEE, June 2022, pp. 6845–6855.
- [25] B. Calli, A. Singh, A. Walsman, S. Srinivasa, P. Abbeel, and A. M. Dollar, "The YCB object and Model set: Towards common benchmarks for manipulation research," in *2015 International Conference on Advanced Robotics (ICAR)*, July 2015, pp. 510–517.
- [26] E. Coumans and Y. Bai, "Pybullet, a python module for physics simulation for games, robotics and machine learning," 2016.
- [27] J.-B. Mouret and J. Clune, "Illuminating search spaces by mapping elites," Apr. 2015.
- [28] B. Mildenhall, P. P. Srinivasan, M. Tancik, J. T. Barron, R. Ramamoorthi, and R. Ng, "NeRF: Representing Scenes as Neural Radiance Fields for View Synthesis," Aug. 2020.